

## Apramycin recognition by the human ribosomal decoding site

Thomas Hermann<sup>a,\*</sup>, Valentina Tereshko<sup>b,1</sup>, Eugene Skripkin<sup>b,2</sup>, Dinshaw J. Patel<sup>b,\*</sup>

<sup>a</sup> Department of Chemistry and Biochemistry, University of California, San Diego, La Jolla, CA 92093, USA

<sup>b</sup> Structural Biology Program, Memorial Sloan-Kettering Cancer Center, New York, NY 10021, USA

Submitted 31 October 2006; revised 7 November 2006

Available online 29 January 2007

(Communicated by M. Lichtman, M.D., 7 November 2006)

### Abstract

Aminoglycoside antibiotics bind specifically to the bacterial ribosomal decoding-site RNA and thereby interfere with fidelity but not efficiency of translation. Apramycin stands out among aminoglycosides for its mechanism of action which is based on blocking translocation and its ability to bind also to the eukaryotic decoding site despite differences in key residues required for apramycin recognition by the bacterial target. To elucidate molecular recognition of the eukaryotic decoding site by apramycin we have determined the crystal structure of an oligoribonucleotide containing the human sequence free and in complex with the antibiotic at 1.5 Å resolution. The drug binds in the deep groove of the RNA which forms a continuously stacked helix comprising non-canonical C•A and G•A base pairs and a bulged-out adenine. The binding mode of apramycin at the human decoding-site RNA is distinct from aminoglycoside recognition of the bacterial target, suggesting a molecular basis for the actions of apramycin in eukaryotes and bacteria.

© 2007 Elsevier Inc. All rights reserved.

**Keywords:** Aminoglycoside antibiotics; Neomycin; Ribosomal decoding site; RNA; X-ray crystallography

### Introduction

The ribosome is a target for many antibiotics that interfere with bacterial protein synthesis by binding to ribosomal RNA components (rRNA) [1,2]. Aminoglycoside antibiotics interact with the decoding site (A site) in 16S rRNA and thereby decrease the fidelity of translation [3]. Structural studies using NMR and X-ray crystallography have revealed the molecular basis for bacterial target discrimination of the natural products which share a common 2-deoxystreptamine (2-DOS) scaffold involved in RNA recognition [2]. Apart from containing an unusual pyrano-pyranose sugar [4], the antibiotic apramycin is unique among the aminoglycosides for several reasons. First, apramycin achieves antibacterial specificity by glycoside substitution of the 2-DOS at the 4-position

only while other decoding-site binding aminoglycoside antibiotics show either 4,5- or 4,6-disubstitution pattern [5]. Second, the primary effect of apramycin is inhibition of elongation by blocking ribosome translocation, in contrast to the disubstituted 2-DOS aminoglycosides which induce miscoding during translation [6]. Third, unlike most other aminoglycoside antibiotics, apramycin has been reported to bind with similar affinities to both the bacterial and eukaryotic (human cytoplasmic) decoding-site RNAs (Fig. 1) [7].

The latter finding, which is confirmed by our experiments reported here, is particularly puzzling as key residues required for apramycin recognition by the bacterial RNA are different in the eukaryotic sequence. We have recently determined the three-dimensional structure of apramycin bound to the bacterial decoding site [8]. Important interactions of apramycin involve hydrogen bonds between the bicyclic sugar II and A1408 in the bacterial target and contacts of sugar III to G1491. In the eukaryotic sequence, these residues are G1408 and A1491, which are not suitable to engage in the same interactions with the antibiotic. To elucidate molecular recognition of the eukaryotic decoding site by apramycin, we have determined by X-ray crystallography the three-dimensional structure of the

\* Corresponding authors.

E-mail addresses: [tch@ucsd.edu](mailto:tch@ucsd.edu) (T. Hermann), [pateld@mskcc.org](mailto:pateld@mskcc.org) (D.J. Patel).

<sup>1</sup> Current address: Department of Biochemistry and Molecular Biology, University of Chicago, Chicago, IL 60637, USA.

<sup>2</sup> Current address: Rib-X Pharmaceuticals, New Haven, CT 06511, USA.

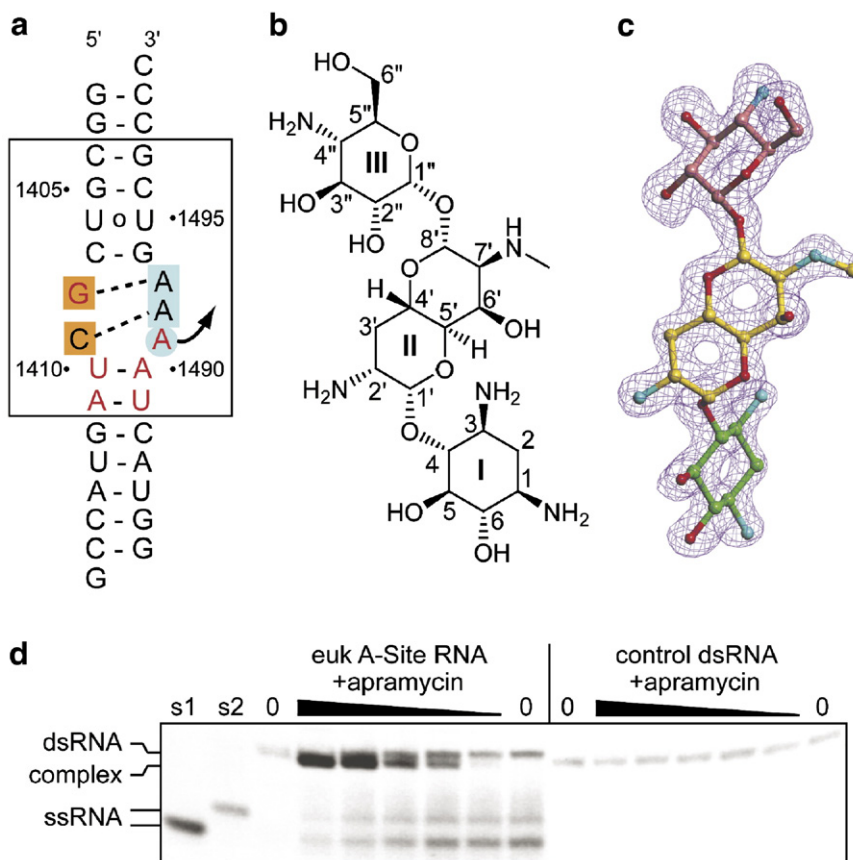


Fig. 1. Apramycin binding to the human ribosomal decoding site (A-site). (a) Secondary structure of the oligonucleotide used for crystallization. The sequence of the human A-site RNA is boxed. Residues that are distinct for the human versus the bacterial sequence are in red. Numbering is adapted from the bacterial *Escherichia coli* sequence. Base-pair formation of G1408•A1493, C1409•A1492, and looping-out of A1491 from the RNA at the internal loop is indicated as observed in the crystal. (b) Structure of apramycin, a unique aminoglycoside antibiotic that contains a terminal 2-deoxystreptamine moiety (ring I) and a bicyclic pyrano-pyranose (ring II). (c)  $2F_o - F_c$  electron density map of apramycin in the crystal contoured at  $1.0\sigma$ . (d) Gel shift experiments demonstrating specific binding of apramycin to the human target RNA. The antibiotic forms a specific complex with the A-site oligonucleotide (left) but not with double-stranded control RNA up to a 4-fold stoichiometric excess (right). The control RNA was derived from the A-site construct by replacing three adenines at positions 1491–1493 with one G and one C, leading to formation of C1409-G and G1408-C pairs instead of the internal loop. Lanes with RNA alone are marked by “0”. Calculated stoichiometric equivalents of 4.0, 2.0, 1.0, 0.5 and 0.25 apramycin/RNA were used. s1 and s2 indicate lanes with the individual RNA single strands that constitute the A-site construct.

antibiotic complexed to a model oligonucleotide containing the human cytoplasmic rRNA target (Fig. 1). For comparison, we have also solved the crystal structure of the unliganded RNA. Similar constructs have been used before for crystallographic structure determination of aminoglycoside–RNA complexes and proved to represent authentic models of the ribosomal decoding site [9,10]. Westhof and coworkers have recently reported a three-dimensional structure of a complex between apramycin and a model RNA that contained the sequences of two human decoding sites [11].

## Materials and methods

### RNA synthesis

Oligoribonucleotides were chemically synthesized from phosphoramidites, purified by polyacrylamide gel electrophoresis and annealed by heating to 75 °C and snap cooling on ice in 5 mM sodium cacodylate buffer, pH 6.5.

### Apramycin binding tests by gel electrophoresis

RNA (50  $\mu$ M concentration) was incubated at room temperature with apramycin sulfate (Sigma, St. Louis, MO) in cacodylate buffer for 5 min. Samples were analyzed by electrophoresis on native 10% polyacrylamide gels in TBE buffer (tris-(hydroxymethyl)-aminomethane/borate/EDTA) and visualized by ethidium bromide staining.

### RNA crystallization

RNA crystals were grown at 20 °C over 3–4 days by vapor diffusion in hanging drops mixed from equal volumes of 0.3 mM RNA (unliganded or apramycin complex) and precipitant buffer containing 50 mM sodium 2-morpholinoethanesulfonate (MES) buffer (pH 5.6), 15–20% 2-methyl-2,4-pentanediol (MPD), and 20–40 mM magnesium acetate. Prior to freezing for X-ray analysis, crystals were briefly soaked in precipitant buffer containing 30% MPD.

Table 1  
Crystal data, collection and refinement statistics

	Free RNA	Apramycin complex
<i>Crystal data</i>		
Space group	<i>P</i> 2 <sub>1</sub> 2 <sub>1</sub> 2 <sub>1</sub>	<i>P</i> 2 <sub>1</sub> 2 <sub>1</sub> 2 <sub>1</sub>
Unit cell <i>a</i> , <i>b</i> , <i>c</i> [Å]	28.16, 36.42, 87.33	28.31, 36.69, 86.68
Asymmetric unit, residues	33	33
H <sub>2</sub> O	72	165
Ions	None	2 Mg <sup>2+</sup> 1 SO <sub>4</sub> <sup>2-</sup>
<i>Data collection</i>		
X-ray source	BNL-X9A	BNL-X9A
Resolution range [Å]	20–2.40	20–1.50
Unique reflections	3649	13,865
Completeness [%]	95.6	92.7
<i>Refinement</i>		
<i>R</i> -factor	0.209	0.199
<i>R</i> <sub>free</sub>	0.252	0.227
R.m.s. deviation:		
Bond length [Å]	0.014	0.015
Bond angles [°]	1.64	1.53

### Structure analysis

X-ray diffraction data of frozen RNA crystals were collected at the beamline NSLS-X9A of the Brookhaven National Laboratory, and processed with the HKL package (crystallographic statistics are summarized in Table 1). Initial phases were obtained by molecular replacement using AMORE [12] with a standard A-form RNA duplex in which the nucleotides A1490–A1493 of the internal loop were omitted and the U1406–U1495 pair was initially replaced by a Watson–Crick A–U base pair. The initial model was completed and refined by adjusting the placement in the electron density map for the correct helical periodicity after visual inspection and repeated rounds of manual rebuilding, followed by geometry and B-factor refinement with CNS [13] (refinement statistics are summarized in Table 1). The coordinates of the unliganded RNA and complex have been deposited (PDB accession codes 2OE6 and 2OE5, respectively).

### Results and discussion

Gel-shift analysis confirmed specific binding of apramycin to an oligonucleotide containing the human decoding-site sequence, which was also used for cocrystallization (Fig. 1d). Complex formation was observed for the decoding-site construct but not for a control RNA lacking the internal loop, thus ruling out the possibility that the drug binds promiscuously to double-stranded RNA and confirming earlier reports of specific apramycin binding to the human target [7].

The crystal structure of the human decoding site was determined at 1.50 Å resolution for the apramycin complex and at 2.40 Å for the unliganded RNA (see Materials and methods). In both the free and complexed structures RNA helices pack by coaxial stacking which is facilitated by intermolecular base-pair formation of the terminal-overhanging

G and C nucleotides and by binding of a Mg<sup>2+</sup> ion that bridges consecutively stacked helices involving contacts of the metal hydration shell to G1402 in one helix and G1417 in the other (Fig. 2).

The internal loop of the eukaryotic decoding site in the apramycin complex is organized by regular stacking of bases along one strand (U1406 to C1409) to which adenines of the adenosine-rich strand (A1491–U1495) are docked, forming non-canonical G1408•A1493 and C1409•A1492 base pairs (Figs. 2b, c, d). The G1408•A1493 pair is in a *trans* sugar-edge/Hoogsteen configuration, stabilized by two hydrogen bonds of the exocyclic amino group of G1408 to the N7 atom and the phosphate group of A1493. A similar geometry has been described for a sheared G•A pair in the hammerhead ribozyme. The C1409•A1492 pair adopts a *cis* sugar-edge/Watson–Crick arrangement involving a hydrogen bond between the exocyclic amino group of C1409 and the N3 atom of A1492, as well as contacts of the O2 and N3 atoms in C1409 and the 2'-OH group of A1492. The exocyclic amino group of A1492 forms also a hydrogen bond with the phosphate group of A1491, which itself is bulged out from the helix and involved in intermolecular stacking contacts of neighboring RNA molecules in the crystal. Surprisingly, the geometry of the decoding-site internal loop is essentially identical in the structure of the apramycin complex and the free RNA (rmsd=0.9 Å), as well as in another crystal structure of the eukaryotic decoding site that has recently been reported by the Westhof group [14]. Specifically, the geometry of the unusual G1408•A1493 and C1409•A1492 base pairs as well as the bulged-out A1491 are virtually identical in the free and apramycin-bound RNA. In contrast to the bacterial target, in which A1492 and A1493 undergo a dramatic conformational change upon binding of aminoglycosides [8,9], apramycin binding to the eukaryotic decoding site merely stabilizes a conformational state of the unliganded eukaryotic RNA.

Apramycin binds within the deep (major) groove of the RNA, with the pyranose ring III oriented towards the internal loop region and the pyrano-pyranose ring (II) aligned with RNA base edges (Fig. 3). Unlike ring II, which is sandwiched in the deep groove between the backbone of opposite strands, pyranose III is accommodated in a perpendicular fashion within the distorted deep groove of the decoding-site internal loop, widened by the G1408•A1493 and C1409•A1492 pairs and the bulged-out A1491. Contact sites of rings II and III of apramycin with the RNA are located within the internal loop and the flanking stem whereas the 2-deoxystreptomine (2-DOS) ring I interacts exclusively with nucleotides in the canonically paired RNA stem. A tight network of direct and water-mediated hydrogen bonds anchors the aminoglycoside at the binding site (Fig. 3b). Extensive intermolecular contacts involve ring III which engages each of its exocyclic hydroxyl and amino groups in two hydrogen bonds, either directly to the RNA or to water. A fully hydrated magnesium ion is found bound in the deep groove just below apramycin pyranose III (Figs. 2 and 3a). The cation hydration shell participates in hydrogen bonds to water molecules located at the base edges of G1408 and C1409 as well as to apramycin. Due to the lower resolution limit of the unliganded RNA structure, we could not confirm if magnesium

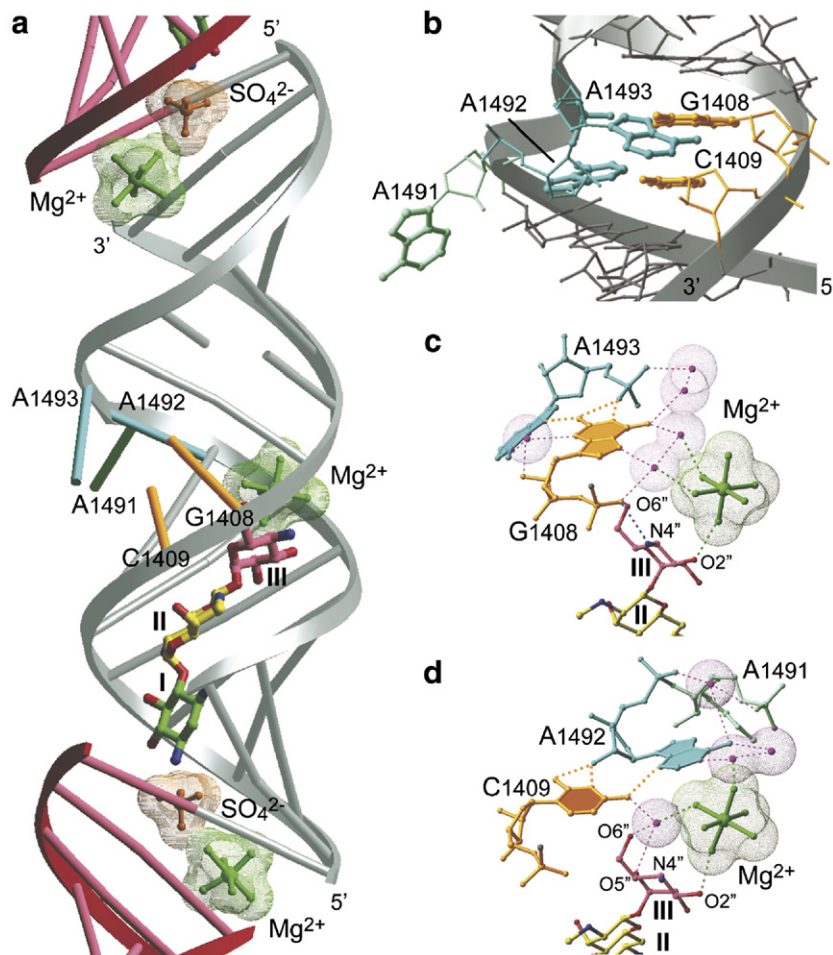


Fig. 2. Structure of the human A-site RNA. (a) Overall view of the A-site oligonucleotide in complex with apiramycin bound in the major (deep) groove. Neighbor oligonucleotides that stack coaxially in the crystal and form intermolecular G–C base pairs via the terminally overhanging residues are shown in red. (b) Conformation of the A-site internal loop in both the apiramycin-bound and free A-site RNA (drug not shown). (c) Interactions of the G1408•A1493 base pair involving apiramycin, a magnesium ion and water molecules (magenta spheres). (d) Interactions of the C1409•A1492 base pair. The base-pairing geometry for both the G1408•A1493 and C1409•A1492 pairs are identical in the structure of the apiramycin-bound and unliganded RNA.

is also bound to the free RNA. The observed interactions of the metal ion with apiramycin suggest, however, that magnesium is not bound at the same location in the free RNA and that it is the drug binding to the RNA that creates the observed magnesium binding site.

Despite intimate contact between apiramycin and the RNA, the drug binding site is rather open. Upon RNA binding, only ~50% of the surface area of apiramycin is buried, roughly corresponding to the ~40% surface burial of the drug in complex with the bacterial decoding site. Comparison of the bacterial and eukaryotic decoding-site complexes of apiramycin reveals very distinct binding modes for the two different targets. In the crystal structure of the bacterial decoding-site complex [4], apiramycin interacts extensively with nucleotides of the internal loop, thereby displacing two adenine residues (A1492, A1493) from the deep groove. The adenine conformational changes induced by drug binding to the bacterial target have been linked to the mechanism of action of the aminoglycoside antibiotics and corresponds to a “standard” binding mode observed for several other aminoglycosides [2,3,9,15,16]. In the

crystal structure of the bacterial 30S ribosomal subunit, the A1492 and A1493 residues adopt multiple conformations, indicative for their flexibility in the absence of mRNA–tRNA hybrid or drugs [15,17].

Comparison of the human decoding site complex of apiramycin described here (solved at 1.5 Å resolution) with the three-dimensional structure of the decoding-site complex determined by the Westhof group (solved at 2.8 Å resolution) [11] reveals a surprising dissimilarity of the ligand binding position despite an overall high similarity of the RNA structures. The base pairing arrangement within the decoding-site loop and orientation of residues that are extruded from the RNA helix (A1491 and A1493) are essentially conserved between the Westhof structure and the complex described here. In contrast, while apiramycin forms contacts mainly to residues immediately flanking the decoding-site loop in the complex structure described here, in the Westhof structure, the ligand binds to the RNA at a position shifted by about five residues. As a consequence, the bicyclic pyrano-pyranose ring of the aminoglycoside (ring II) is centered approximately at the edge

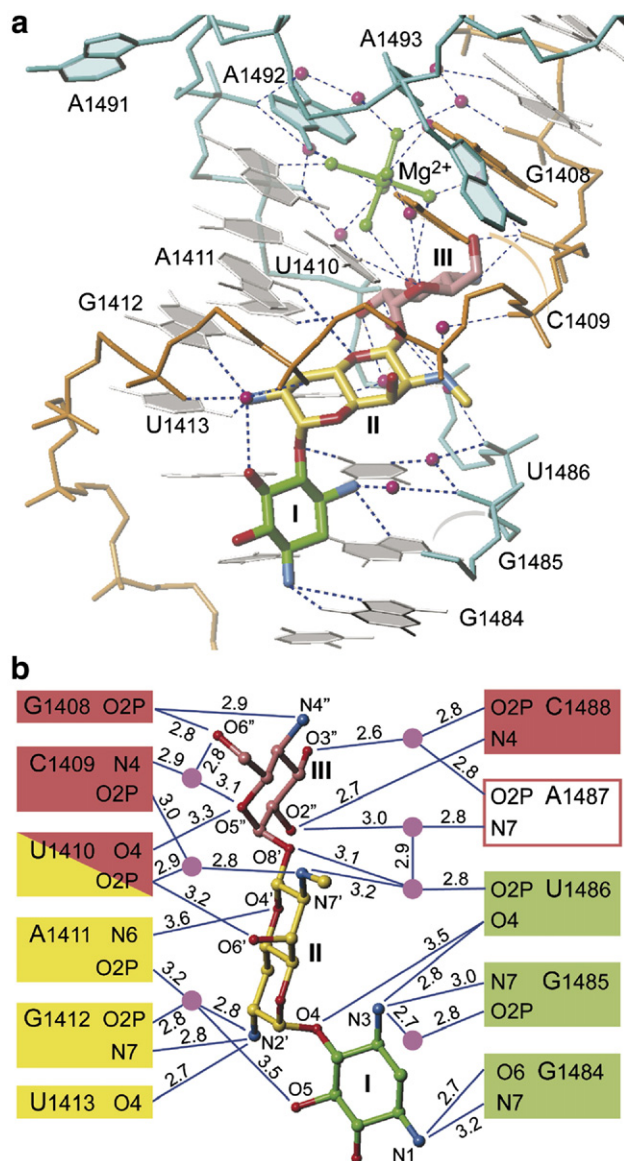


Fig. 3. Interactions of apramycin with the human A-site RNA. (a) View into the major (deep) groove at the antibiotic binding site that extends from the A-site internal loop into the Watson–Crick-paired region below. Potential hydrogen-bond interactions are indicated. Water molecules are shown as magenta spheres. (b) Intermolecular distances between hydrogen-bond donors and acceptors in the apramycin complex. Color coding of RNA residues corresponds to regions that interact with rings I, II, and III of the aminoglycoside. Filled boxes indicate direct interactions, outlined boxes show water-mediated contacts.

of the G1412–C1488 pair in our structure while it is located at C1407–G1494 in the Westhof structure. Binding of apramycin to either of the two sites would lock the architecture of the decoding site in a conformation that prevents proper function in the decoding process [11]. The coexistence of distinct binding sites for apramycin within the largely unchanged three-dimensional architecture of the same RNA target provides yet another example of the promiscuous RNA affinity of aminoglycosides and the challenges for drug design directed at the decoding-site target.

In conclusion, the three-dimensional structure of the eukaryotic decoding-site complex of apramycin reveals a unique

binding mode of the antibiotic to the human target RNA that is distinct from the structure of bacterial decoding-site complexes of aminoglycosides including apramycin. Unlike in the bacterial complexes, in which binding of the drugs induces a conformational change of two adenines that interferes with the ribosomal decoding process, apramycin seems to stabilize a pre-existing conformational state of the free eukaryotic decoding-site RNA. As we have shown here, the crystal structure of the free RNA is virtually identical to that of the apramycin complex. Importantly, apramycin binding to the native conformation of the eukaryotic decoding-site is a specific event and not a result of promiscuous interactions. Since apramycin also interacts specifically with the bacterial RNA target, yet in a different binding mode but with comparable affinity, this natural product represents the first example of an RNA-directed ligand that recognizes its cognate target in a species-specific fashion.

### Acknowledgments

This paper is based on a presentation at the Focused Workshop “RNA Chemistry Meets Biology” sponsored by The Leukemia and Lymphoma Society in Sweden, September 29–30, 2006. This work was supported by a NIH grant to D.J.P. We thank P.D. Jeffrey for assistance with data processing and A. Serganov for helpful discussions.

### References

- [1] A. Yonath, Antibiotics targeting ribosomes: resistance, selectivity, synergism and cellular regulation, *Annu. Rev. Biochem.* 74 (2005) 649–679.
- [2] T. Hermann, Drugs targeting the ribosome, *Curr. Opin. Struct. Biol.* 15 (2005) 355–366.
- [3] J.M. Ogle, V. Ramakrishnan, Structural insights into translational fidelity, *Annu. Rev. Biochem.* 74 (2005) 129–177.
- [4] S. O’Connor, L.K. Lam, N.D. Jones, M.O. Chaney, Apramycin, a unique aminocyclitol antibiotic, *J. Org. Chem.* 41 (1976) 2087–2092.
- [5] R. Ryden, B.J. Moore, The in vitro activity of apramycin, a new aminocyclitol antibiotic, *J. Antimicrob. Chemother.* 3 (1977) 609–613.
- [6] S. Perzynski, M. Cannon, E. Cundliffe, S.B. Chahwala, J. Davies, Effects of apramycin, a novel aminoglycoside antibiotic on bacterial protein synthesis, *Eur. J. Biochem.* 99 (1979) 623–628.
- [7] R.H. Griffey, S.A. Hofstadler, K.A. Sannes-Lowery, D.J. Ecker, S.T. Crooke, Determinants of aminoglycoside-binding specificity for rRNA by using mass spectrometry, *Proc. Natl. Acad. Sci. U. S. A.* 96 (1999) 10129–10133.
- [8] Q. Han, Q. Zhao, S. Fish, K.B. Simonsen, D. Vourloumis, J.M. Froelich, D. Wall, T. Hermann, Molecular recognition by glycoside pseudo base pairs and triples in an apramycin–RNA complex, *Angew. Chem. Int. Ed. Engl.* 44 (2005) 2694–2700.
- [9] Q. Vicens, E. Westhof, Molecular recognition of aminoglycoside antibiotics by ribosomal RNA and resistance enzymes: an analysis of X-ray crystal structures, *Biopolymers* 70 (2003) 42–57.
- [10] F. Zhao, Q. Zhao, K.F. Blount, Q. Han, Y. Tor, T. Hermann, Molecular recognition of RNA by neomycin and a restricted neomycin derivative, *Angew. Chem. Int. Ed. Engl.* 44 (2005) 5329–5334.
- [11] J. Kondo, B. Francois, A. Urzhumtsev, E. Westhof, Crystal structure of the homo sapiens cytoplasmic ribosomal decoding site complexed with apramycin, *Angew. Chem. Int. Ed. Engl.* 45 (2006) 3310–3314.
- [12] J. Navaza, AMoRe: an automated package for molecular replacement, *Acta Crystallogr., A* 50 (1994) 157–163.
- [13] A.T. Brunger, P.D. Adams, G.M. Clore, W.L. DeLano, P. Gros, R.W. Grosse-Kunstleve, J.S. Jiang, J. Kuszewski, M. Nilges, N.S. Pannu, R.J. Read, L.M. Rice, T. Simonson, G.L. Warren, *Crystallography and NMR*

- system: a new software suite for macromolecular structure determination, *Acta Crystallogr., Sect. D: Biol. Crystallogr.* 54 (1998) 905–921.
- [14] J. Kondo, A. Urzhumtsev, E. Westhof, Two conformational states in the crystal structure of the *Homo sapiens* cytoplasmic ribosomal decoding A site, *Nucleic Acids Res.* 34 (2) (2006) 676–685.
- [15] J.M. Ogle, D.E. Brodersen, W.M. Clemons Jr., M.J. Tarry, A.P. Carter, V. Ramakrishnan, Recognition of cognate transfer RNA by the 30S ribosomal subunit, *Science* 292 (5518) (2001) 897–902.
- [16] A.P. Carter, W.M. Clemons, D.E. Brodersen, R.J. Morgan-Warren, B.T. Wimberly, V. Ramakrishnan, Functional insights from the structure of the 30S ribosomal subunit and its interactions with antibiotics, *Nature* 407 (6802) (2000) 340–348.
- [17] B.T. Wimberly, D.E. Brodersen, W.M. Clemons Jr., R.J. Morgan-Warren, A.P. Carter, C. Vonrhein, T. Hartsch, V. Ramakrishnan, Structure of the 30S ribosomal subunit, *Nature* 407 (6802) (2000) 327–339.